

Analyzing Proton Spectroscopic Factors from $(d, {}^3\text{He})$, $({}^3\text{He}, d)$, and (d, n) transfer reactions

Rebecca Habas,
University of Rochester

Supervisor: Professor Betty Tsang
National Superconducting Cyclotron Laboratory
Michigan State University

Abstract

We have reanalyzed ground state to ground state proton spectroscopic factors for selected nuclei by analyzing previous measurements of the angular distributions from $(d, {}^3\text{He})$, $({}^3\text{He}, d)$, and (d, n) transfer reactions. In published literature, spectroscopic factors generally show large fluctuations, due to different potential models and input parameters, making it difficult to extract the nuclear structure information. It has been shown previously that using systematic and consistent model parameters can give good agreement between theory and experimental data for neutron spectroscopic factors [1,2]. We extended this method to proton transfer reactions, and found that the data is generally self-consistent to within 20%.

Introduction:

In 1949, Mayer and Jensen independently proposed the successful Shell Model to describe nuclear structure. The original nuclear shell model, also known as the independent particle model, stipulates that nucleons move independently inside a potential $V(r)$. The potential is due to the average effect of all other nucleons on any particular nucleon. Analogous to the electron shell model, each energy level, or shell, fills according to the Pauli exclusion principle, and once one level is full, the next nucleon fills the next lowest energy level. Protons and neutrons fill separate shells, independent of each other. The nuclear shell model differs from the electron shell model, however, in the ordering of the shells, resulting in the different values of the magic numbers as shown in Fig. 1.

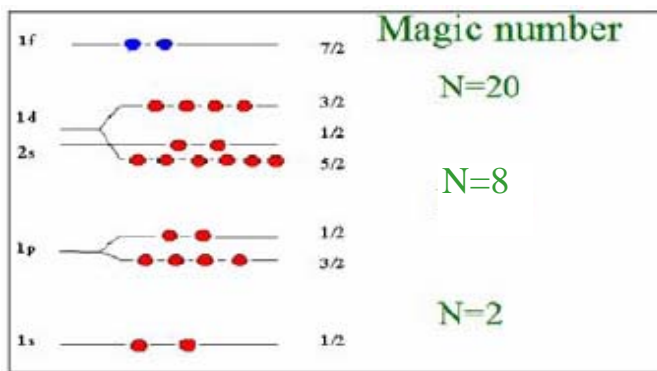


Figure 1. The Shell Model structure for neutrons in ^{42}Ca .

If the number of neutrons or protons equals a magic number (2, 8, 20, 28, 50, 82, 126), then the nucleus exhibits certain characteristics: the isotope is more stable, the binding energy per particle is higher, and there exists a greater number of isotopes, for example. If both the proton number and the number of neutrons equals a magic number the isotope is called doubly magic, and it is even more tightly bound. An example is ^{40}Ca . The closed shells essentially form an inert core, and the properties of the isotope are given by the valence nucleons. Transfer reactions, like those studied in this reaction, probe the surface structure of the isotope.

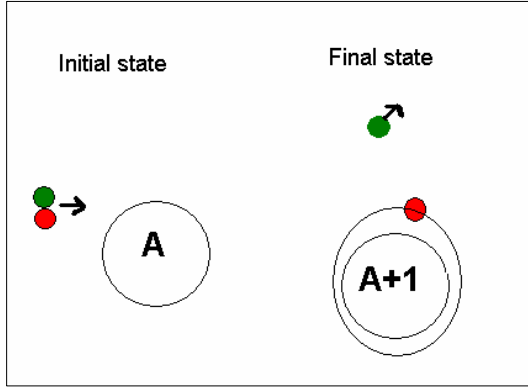


Figure 2. A stripping reaction (the particle is stripped off the incident particle). Only the outer level is involved in the reaction.

Theoretical Spectroscopic Factor:

The spectroscopic factor is a measure of how well one can describe the single particle nature of valence nucleons, and is important because this number provides the most basic test to the shell model. In stripping reactions, the spectroscopic factor is related to the expansion of the wave function for a specific state in the target nucleus with A nucleons Ψ_i^A , in terms of a summation over the complete set of states in the final nucleus with $A+1$ nucleons Ψ_f^{A+1} :

$$\Psi_i^A = \sum_f \Phi_f^i(\vec{r}) \Psi_f^{A+1}$$

where $\Phi_f^i(\vec{r}) = \langle \Psi_f^{A+1} | \Psi_i^A \rangle$ is the overlap integral.

The theoretical spectroscopic factor S is then defined as the square of the normalization of the overlap integral between the wave function of the valence nucleons in the state of the target nucleus and the residual nucleus [2,3], given by:

$$S = (\int \Phi_f^i(\vec{r}) d\tau)^2$$

Experimental spectroscopic factor:

The experimental spectroscopic factor is the ratio of the experimental differential cross section over the theoretical differential cross section, which is dependent on the reaction model. Both quantities are measured or calculated as functions of the angle θ , as illustrated in Figure 2.

$$S_{\text{exp}} = \frac{\left(\frac{d\sigma}{d\Omega}\right)_{\text{exp}}}{\left(\frac{d\sigma}{d\Omega}\right)_{\text{theory}}}$$

The differential cross section represents the probability of the particles scattered per unit time within the element of solid angle in the direction with respect to the incident beam.

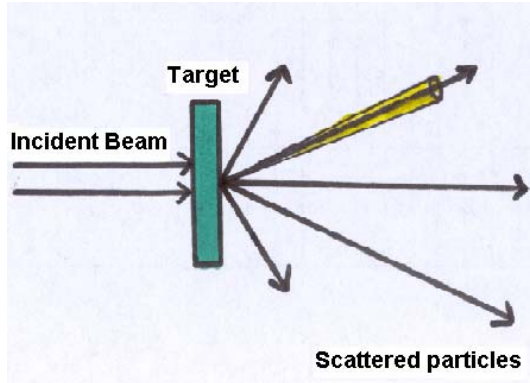


Figure 3. A diagram of the cross section, as a function of angle.

Within the context of the shell model, the spectroscopic factor measures how well the nucleus can be described as a single particle plus a core. Taking the ratio of the experimental spectroscopic factor over the spectroscopic factor predicted by the shell model gives two possible results. If $S_{\text{exp}}/S_{\text{SM}} = 1$, then the orbital description of the shell model is accurate. If instead $S_{\text{exp}}/S_{\text{SM}} > 1$, then the valence nucleons occupy more than one orbit.

A survey of published spectroscopic factors for any given isotope shows large fluctuations. This is due in part to different definitions for the spectroscopic factor, and the use of different potentials and input parameters. The objective of this project is to adopt a standard set of input parameters, and reanalyze previously published spectroscopic factors using a systematic and consistent method to extract more accurate values for the spectroscopic factor. In order to understand the structure of rare isotopes away from the valley of stability, it is important to first understand the structure of stable isotopes. Thus any ambiguities in the spectroscopic factors for these stable nuclei first need to be identified and then explained, which first requires an accurate measurement of the spectroscopic factors.

Analysis:

In the past 40 years, there have been many studies of single particle stripping and pickup reactions. We searched the literature for published figures of angular distributions from (d,³He), (³He,d), and (d,n) reactions, which we then digitized. As mentioned previously, we also focused solely on the ground state to ground state transfers. Figure 4 shows a typical plot. The shape of the curve depends on both the l-value and the energy per nucleon of the incident particle. The theoretical curves were generated by the program TWOFNR, which was provided by Jeff Tostevin from the University of Surrey. This code is based on the Distorted Wave Born Approximation (DWBA), which assumes a direct, single-step transfer reaction. In the general reaction A(a,b)B, the transition amplitude given by the DWBA model can be written as:

$$T = \iint \chi^{(-)}(\vec{\kappa}_f, \vec{r}_b) \langle \Phi_B | V | \Phi_A \rangle \chi^{(+)}(\vec{\kappa}_i, \vec{r}_a) d\vec{r}_a d\vec{r}_b$$

where $\chi^{(-)}$ and $\chi^{(+)}$ are the wave functions describing the elastic scattering of the scattered and incident particles, respectively,

Φ_B and Φ_A are the wave functions of the final and initial nuclei, respectively,

κ is the momentum

r represents the relative coordinates, and

V is the interaction potential

The theoretical curve was normalized to the experimental data. We restricted the curve to the first peak, because the backward angles are more susceptible to inelastic scattering and higher order effects. As can be seen in figure 4., the fit of the first peak is good, but the second peak already deviates from the theoretical curve due to these other effects.

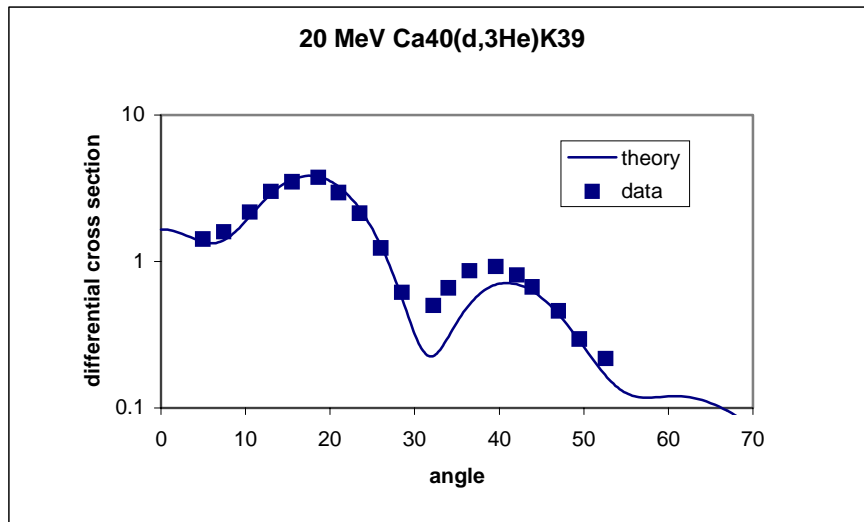


Figure 4. A typical plot of the angular distributions.

To avoid any inconsistencies in the extracted spectroscopic factors, we used a standard set of parameters. The Chapel-Hill global optical potential was adopted for both the deuteron and neutron in the (d,n) reactions. The Johnson-Soper adiabatic potential accounts for the deuteron breakup in the field. This potential was not applicable for the other two reactions. Instead we used the Daehnick global potential for deuterons and the Bechetti-Greenlees potential for ^3He . In all cases, we chose a local energy approximation for finite range effects and included non-locality corrections in both the entrance and exit channels.

^3He potential	Bechetti-Greenlees
Deuteron potential {(d, ^3He) and (^3He ,d)}	Daehnick Global
Deuteron potential (d,n)	Adiabatic potential-Chapel Hill
Neutron potential	Chapel Hill
Hulthen finite range factor	0.7462 {(d, ^3He) and (^3He ,d)} 0.7457 (d,n)
n-binding potential	Woods-Saxon r0=1.25, a=0.65
Vertex Constant D_0^2	25600 {(d, ^3He) and (^3He ,d)} 15006.25 (d,n)
Non-locality potentials	deuteron: 0.85 fm (d,n) 0.54 {(d, ^3He) and (^3He ,d)} ^3He : 0.25 fm neutron: 0.85 fm

Table 1. Summary of the input parameters

In addition, the incident energies we examined were generally between 10-100 MeV. At lower incident energies, resonance and compound nuclear effects dominate, and the global potentials we adopted may not be valid at energies above 100 MeV. In some reactions with little data, experimental results with incident energies outside this region were analyzed, but the results are inherently more uncertain.

Results and Discussion

In the present work, we analyzed selected nuclei from (d, ^3He), (^3He ,d), and (d,n) reactions. The particular isotopes were selected because the nuclear structure is believed to be particularly well understood or due to the amount of available data. The preliminary results are shown in Table 2. In this table the isotopes listed are the final state isotopes, which here refers to the isotopes in the reaction with the highest A value. In calculating the average spectroscopic

factor for each reaction, points with likely measurement errors were excluded, as were measurements with missing data at the forward angles. The extracted values are weight-averaged with respect to the number of points used when normalizing the theoretical curve to the data points. This was used to place less emphasis on the extracted values from poor data or data with only one or two data points on the shoulder of the first peak. Fits to such data are dubious at best, due to the influence of higher order effects. Multiple sources of data from the same work were averaged separately, and this value was averaged with the rest, to ensure that the influence of any errors in a single work is minimized, as well. The number of references used for each isotope is also included. This number is generally much smaller than the number of published works. Many papers did not include the specific angular distributions for which we were searching. A glance at the table will also show that the majority of the data comes from the (d,³He) reactions. There are fewer studies done with the (d,n) and (³He,d) reactions; particularly for (d,n), the studies that are done tend to all focus on a few target isotopes.

Further investigation needs to be done on the sources of discrepancies between data points, particularly and discrepancies between points at the same incident energy. In addition, any data with the extracted spectroscopic factor larger than predicted by the shell model (the heavier nuclei) need a more detailed analysis, and ¹⁴C, which more than likely has a normalization error, was only included for completeness. The values predicted by the simple shell model are given in Table 3. Since isotopes by definition have the same number of protons, there is only one value per element.

In general, the extracted spectroscopic factors are self-consistent, although in a cursory analysis they appear a bit high. Figure 5 shows the scatter of published spectroscopic values (top) and of the spectroscopic factors extracted in a consistent manner in this work (bottom) for ⁴⁰Ca. The scatter of our data is much more consistent within the uncertainties of the experimental measurements, and in general, much lower. ⁴⁰Ca is a doubly magic isotope and has four valence protons, thus one expects it to have a spectroscopic value of four (according to the shell model). Our points are not only more self consistent, within each of the three reactions, but they also reproduce to this theoretical value much better. The blue line in the top plot corresponds to the averaged value compiled by Endt [4]. He completed an earlier compilation and analysis of published spectroscopic factors, however in many instances he relied on personal

isotope	(d, ^3He)	no. of measurements	(^3He ,d)	no. of measurements	(d,n)	no. of measurements	<SF>
^{11}C			2.1	2	1.15	2	1.63
^{12}C	2.73	2	4.01	2	3.13	4	3.32
^{13}C	1.74	3					1.74
^{14}C	15.55	1					15.55
^{15}O			2.82	3	0.67	3	1.75
^{16}O	3.01	5	2.47	2	2.63	2	2.70
^{17}O	1.21	1					1.21
^{29}P			0.88	5	0.45	2	0.88
^{30}P			0.63	2	0.31	1	0.63
^{31}P	1.45	1	0.90	4			1.18
^{32}S	1.41	4	2.19	3	1.78	4	1.80
^{34}S	1.57	1					1.57
^{36}S	2.70	2					2.70
^{40}Ca	3.63	7	4.73	3	3.67	2	4.33
^{41}Ca	2.41	1	1.14	1	0.59	1	1.78
^{42}Ca	2.69	2	2.39	1			2.54
^{43}Ca	0.38	1					0.38
^{44}Ca	2.20	1					2.20
^{46}Ca	3.39	1					3.39
^{48}Ca	2.35	3					2.35
^{47}V			0.15	2			0.15
^{49}V			0.89	2			0.89
^{50}V			1.00	1			1.00
^{51}V	0.94	5	1.13	3			1.03
^{58}Ni	5.35	4					5.35
^{60}Ni	8.65	2	7.93	2			8.82
^{61}Ni	9.71	1					9.71
^{62}Ni	4.57	1					4.57
^{64}Ni	7.67	2					7.67
^{90}Zr	3.25	2	1.93	1			2.59
^{91}Zr	0.79	2					0.79
^{92}Zr	2.25	1					2.25
^{94}Zr	3.15	1					3.15
^{96}Zr	2.62	1					2.62
^{112}Sn	8.01	1					8.01
^{116}Sn	9.53	3	12.84	1			11.19
^{118}Sn	13.63	1					13.63
^{120}Sn	12.54	1					12.54
^{122}Sn	11.74	1					11.74
^{124}Sn	11.47	1					11.47
^{142}Nd	4.10	1	3.13	1			3.62
^{206}Pb	2.61	3	6.69	1			4.65
^{208}Pb	2.25	4					2.25

Table 2. The spectroscopic factors extracted from each reaction studied and the overall average spectroscopic factor obtained in the current analysis.

Element	S_{SM}
C	4
O	2
P	6
S	2
Ca	4
V	3
Ni	8
Zr	2
Sn	10
Nd	2
Pb	2

Table 3. Spectroscopic factors predicted by the Nuclear Shell Model.

communication with the authors, and it is unclear if his treatment of the data was consistent. In addition, his collection of data only extends through 1975; with a larger collection of data that includes newer results, we would expect better trends to emerge. Endt acknowledged that the scatter for ^{40}Ca is particularly bad, and he refused to assign a best value spectroscopic factor to this isotope- thus the line here is the average value of his data (7.26). It is much higher than the theoretical value.

^{40}Ca best shows the usefulness of using a systematic approach to extracting spectroscopic factors. Other isotopes, such as ^{16}O and ^{32}S , have only slightly narrower spreads.

In certain cases, the proton spectroscopic factor can also be compared to the neutron spectroscopic factor. For nuclei with $N=Z$, the proton and neutron structure inside the nucleus is identical, according to the shell model, and therefore probes of the nucleonic structure such as transfer reactions should give the same results. Thus, comparing the two obtained spectroscopic values can add another check to the accuracy and consistency of the results. Table 4 shows the spectroscopic values obtained for each reaction with $N=Z$ studied in this work, the calculated average value, and the neutron spectroscopic factor for comparison. The general agreement between the proton and neutron spectroscopic factors is fair.

Isotope	$\langle SF \rangle$ (d, ^3He)	$\langle SF \rangle$ (^3He , d)	$\langle SF \rangle$ (d, n)	$\langle SF \rangle$	$\langle SF \rangle_{\text{n}}$	$\langle SF \rangle / \langle SF \rangle_{\text{n}}$
^{12}C	2.73	4.01	3.13	3.29	2.98	1.104
^{16}O	3.01	2.74	2.63	2.79	2.23	1.251
^{32}S	1.41	2.19	1.78	1.79	1.46	1.226
^{40}Ca	3.63	4.73	3.67	4.01	4.3	0.933

Table 4. A comparison between the neutron and proton spectroscopic factors, from this work and ref 1.

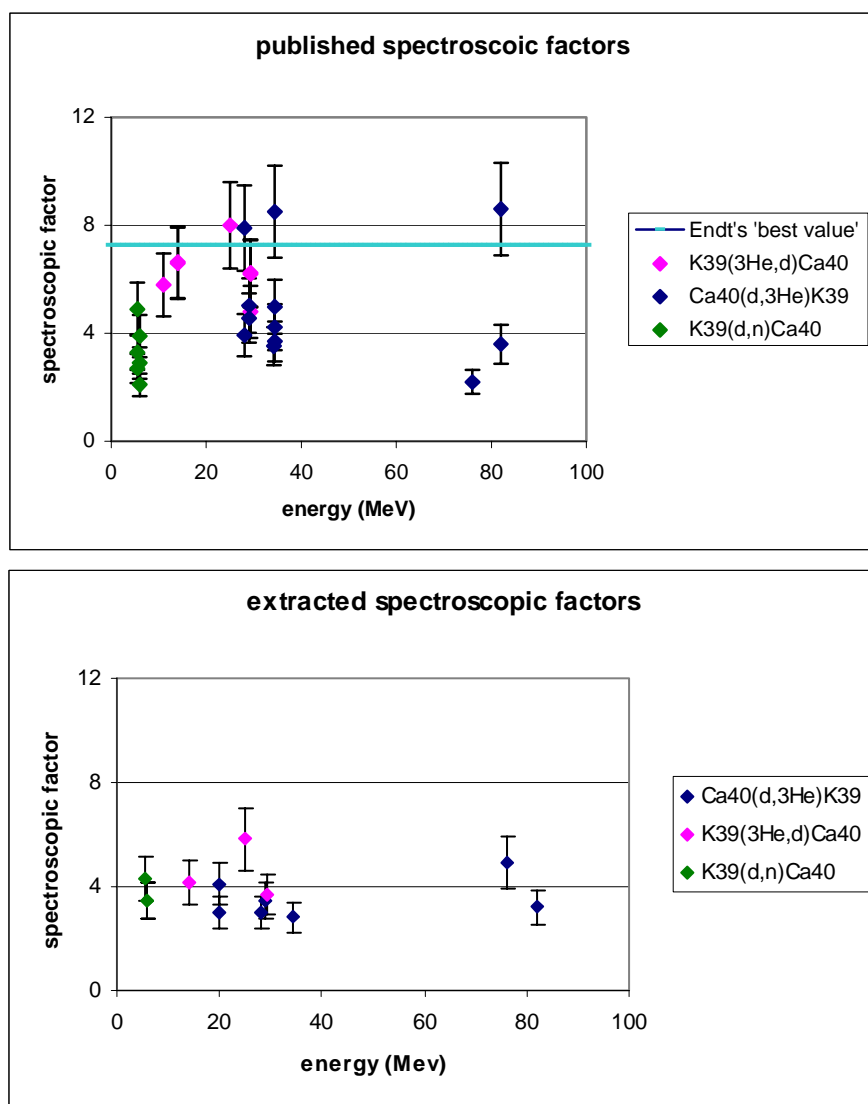


Figure 5. These two plots show the scatter of published (top) and extracted (bottom) spectroscopic factors for ^{40}Ca isotopes. The points extracted in this analysis are more consistent with each other and with the theoretical value of 4.

Conclusion

The spectroscopic factors extracted from each published work generally show surprisingly good agreement with each other. Perfect agreement, while ideal, was not expected. For N=Z nuclei, the extracted proton spectroscopic factors are also consistent with previously extracted neutron spectroscopic factors. Further analysis still needs to be done to quantitatively assign errors associated with the spectroscopic factor of each isotope. Any discrepancies in the data, for example the spectroscopic factor >5 in ^{40}Ca , still need to be satisfactorily explained. In addition, the analysis of the rest of the isotopes for each reaction must be completed, as does all the data for (n,d) transfer reactions. Overall, however, the data extracted in a systematic manner shows good self-consistency, and, where it has already been compared, shows good agreement with theory.

Acknowledgements

I would like to thank Professor Betty Tsang and Jenny Lee for their innumerable help and support with this project. I would also like to thank MSU and the NSCL for hosting the REU program, and the NSF for funding this opportunity.

References

- [1] B. M. Tsang, H.C. Lee, W. Lynch, Survey of Ground State Neutron Spectroscopic Factors From Li to Cr Isotopes, pending publication
- [2] Jenny Lee, Survey of Spectroscopic Factor for Li-Cr Isotopes
- [3] Alex Brown, Some notes on Spectroscopic Factors
- [4] P.M. Endt, Atomic Data and Nuclear Data Tables 19, 23 (1977)